RESEARCH ARTICLE

Non-Darcian-Benard-magneto-surface tension driven convection in an infinite horizontal composite layer in the presence of heat source/sink and non-uniform temperature gradients

Sumithra R [a], Manjunatha N [b,*], Komala B [c]

[a] Department of UG, PG Studies & Research in Mathematics, Government Science College Autonomous, Bengaluru, Karnataka, India
[b] School of Applied Sciences, REVA University, Bengaluru, Karnataka, India
[c] Department of Mathematics, Dayananada Sagar University, Bengaluru, Karnataka, India

* Corresponding author: manjunatha.n@reva.edu.in

Abstract

The physical pattern of the problem consists of an infinite horizontal composite layer, in the presence of uniform heat source/sink in both the layers enclosed by upper adiabatic, lower isothermal boundaries and continuity of heat and heat flux at the interface. The problem of non-Darcian-Benard-magneto-surface tension driven convection is investigated on this composite layer which is subjected to uniform and nonuniform temperature gradients. The eigenvalue, thermal Marangoni number in the closed form is obtained for lower surface rigid, upper surface free with surface tension and with the continuity of normal and tangential stresses and continuity of normal, tangential velocity boundary conditions at the interface. The influence of various parameters on the Marangoni number against thermal ratio is discussed. It is observed that the heat absorption in the fluid layer and the applied magnetic field play an important role in controlling non-Darcian-Benard-magneto-surface tension driven convection.

Keywords: Heat source (sink), thermal ratio, exact method, temperature gradients, adiabatic and isothermal boundaries, magnetic field.

INTRODUCTION

In many situations particularly in geophysics and astrophysics, in works involving crystal growth, maintaining a uniform temperature gradient is a challenge where the occurrence of non-uniform temperature gradients is common. While the instabilities of a fluid in the presence of such gradients is of practical importance, this issue is not given much attention. Furthermore, the occurrence of composite layers is also a reality with not much attention is given. In the study of instabilities, the occurrence of heat absorption and/or heat rejection is common and plays an important role in the convective instabilities. The convective instabilities in the presence of heat source/sink has been widely studied by Rionero and Straughan (1990), Rao and Wang (1991), Rees and Pop (1995), Parthiban and Patil (1997), Khalili and Shivakumara (1998), Herron (2001), Khalili *et al.* (2002), Sankar *et al.* (2006), Joshi *et al.* (2006), Vadasz (2008), Nouri-Borujerdi *et al.* (2008), Grosnan *et al.* (2009), Cookey *et al.* (2010), and Jawdat and Hashim (2010).

Sankar *et al.* (2011a, 2011b) studied the natural convection flows in a vertical annulus filled with a fluid-saturated porous medium when the inner wall is subjected to discrete heating and effect of magnetic field on the combined buoyancy and surface tension driven convection in a cylindrical annular enclosure. Bhadauria (2012) investigated double diffusive convection in a saturated anisotropic porous layer with internal heat source. Sankar *et al.* (2013) studied the natural convection in a vertical annulus filled with a fluid-saturated porous medium, and with internal heat generation subject to a discrete heating from the inner wall. In a recent study, Siddheshwar and Vanishree (2018) have obtained Lorenz and Ginzburg Landau equations for thermal convection in a high porosity medium with heat source. Analysis of fully developed mixed convection in open-ended annuli with viscous dissipation studied by Girish *et al.* (2019). They obtained an excellent agreement between analytical and numerical solutions under limiting conditions.

The idea of using magnetic field to suppress the instabilities has been first introduced by Utech and Fleming (1966) and Chedzey and Hurle (1966) and some recent works on magneto convective instabilities in single fluid/porous layers with different types of fluids along with heat source/sink. Ahmed Kadhim Hussein *et al.* (2016) examined the laminar steady magneto hydrodynamic natural convection in an inclined T-shaped enclosure filled with nanofluids subjected to a uniform heat source numerically by using the finite difference method. The flow of an incompressible Magneto hydrodynamic nanoliquid induced due to unsteady contracting cylinder with uniform heat generation/absorption is investigated numerically through the help of RKF-45 technique by Ramesh *et al.* (2018). Fagbade *et al.* (2018) analyzed MHD natural convection flow of viscoelastic fluid over an accelerating permeable surface with thermal radiation and heat source or sink by spectral homotopy analysis approach and they found that an increase in thermal radiation parameter of the flow produces significant increase in the thermal condition of the fluid temperature.

In their study, Sharma *et al.* (2018) aimed to investigate the effects of heat generation/absorption on MHD mixed convective stagnation point flow along a vertical stretching sheet in the presence of external magnetic field obtained solution by using R-K fourth

order scheme and shooting technique. The following year, Om Prakash Keshri *et al.* (2019) has investigated the effect of internal heat source on magneto stationary convection of couple stress fluid under magnetic field modulation analytically and used weakly nonlinear theory to obtain heat transfer. They found that the couple stress parameter and magnetic Prandtl number destabilize and the Chandrasekhar number has stabilizing effect. The influence of heat source/sink and hall current on MHD flow between vertical alternate conducting walls is studied by Dileep Kumar *et al.* (2020). Naveen and Singh (2020) obtained solutions in closed form of Bessel and modified Bessel functions of order zero for the hydromagnetic natural convective flow between concentric cylinders with heat source/sink. Sumithra *et al.* (2020) have demonstrated the study of Marangoni convection along with the presence of heat sources in both fluid and porous layers of the composite layer. Sumithra and Manjunatha (2020) discussed Benard Magneto Marangoni convection in flow past a densely packed porous layer along with heat sources in both the layers.

The problem of non-Darcian-Benard-magneto-surface tension driven convection is investigated on this composite layer which is subjected to uniform and nonuniform temperature gradients using Brinkman model. Here, an infinite horizontal composite layer in the presence of uniform heat source/sink in both the layers enclosed by upper adiabatic, lower isothermal boundaries is considered. A closed form solution is obtained for the eigenvalue, thermal Marangoni number for upper surface free, with surface tension effects and the lower surface rigid, and with the continuity of normal and tangential stresses and continuity of normal, tangential velocity boundary conditions at the interface. The weightage of diverse parameters on the Marangoni number against thermal ratio is presented.

Mathematical formulation

Consider a horizontal single component, electrically conducting fluid saturated isotropic sparsely packed porous layer of thickness d_m underlying a single component fluid layer of thickness d with an imposed magnetic field intensity H_0 in the vertical z-direction and with heat sources ϕ_m and ϕ, respectively. The lower surface of the porous layer rigid and the upper surface of the fluid layer is free with surface tension effects depending on temperature. A Cartesian coordinate system is chosen with the origin at the interface between porous and fluid layers and the z-axis, vertically upwards.
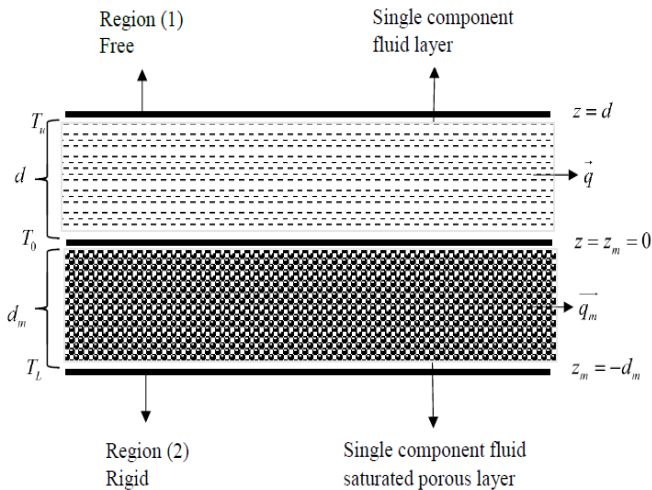
Figure 1. Physical configuration of the problem.

The basic equations for fluid and porous layer respectively governing such a system are

$$\nabla \cdot \vec{q} = 0 \tag{1}$$

$$\nabla \cdot \vec{H} = 0 \tag{2}$$

$$\rho_0 \left[\frac{\partial \vec{q}}{\partial t} + (\vec{q} \cdot \nabla)\vec{q} \right] = -\nabla P + \mu \nabla^2 \vec{q} + \mu_p (\vec{H} \cdot \nabla)\vec{H} \tag{3}$$

$$\frac{\partial T}{\partial t} + (\vec{q} \cdot \nabla)T = \kappa \nabla^2 T + \phi \tag{4}$$

$$\frac{\partial \vec{H}}{\partial t} = \nabla \times \vec{q} \times \vec{H} + \nu_m \nabla^2 \vec{H} \tag{5}$$

$$\nabla_m \cdot \vec{q}_m = 0 \tag{6}$$

$$\nabla_m \cdot \vec{H} = 0 \tag{7}$$

$$\rho_0 \left[\frac{1}{\varepsilon} \frac{\partial \vec{q}_m}{\partial t} + \frac{1}{\varepsilon^2} (\vec{q}_m \cdot \nabla_m)\vec{q}_m \right] = -\nabla_m P_m - \frac{\mu}{K} \vec{q}_m$$
$$+ \mu_m \nabla^2 \vec{q}_m + \mu_p (\vec{H} \cdot \nabla_m)\vec{H} \tag{8}$$

$$A \frac{\partial T_m}{\partial t} + (\vec{q}_m \cdot \nabla_m)T_m = \kappa_m \nabla_m^2 T_m + \phi_m \tag{9}$$

$$\varepsilon \frac{\partial \vec{H}}{\partial t} = \nabla_m \times \vec{q}_m \times \vec{H} + \nu_{em} \nabla_m^2 \vec{H} \tag{10}$$

where $\vec{q} = (u, v, w)$, $\vec{H}$, ρ_0, t, $P = p + \frac{\mu_p H^2}{2}$, μ, μ_p, T, κ, $\nu_m = \frac{1}{\mu_p \sigma}$, σ, ε, μ_m, K, $A = \frac{(\rho_0 C_p)_m}{(\rho_0 C_p)_f}$, C_p, $\nu_{em} = \frac{\nu_m}{\varepsilon}$ are namely the velocity vector, the magnetic field, the fluid density, the time, the total pressure, the fluid viscosity, the magnetic permeability, the temperature of the fluid, the thermal diffusivity of the fluid, the magnetic viscosity, the electrical conductivity, the porosity, the effective viscosity of the fluid in the porous layer, the permeability of the porous medium, the ratio of heat capacities, the specific heat, the effective magnetic viscosity, respectively, and the subscripts 'm' and 'f' refer to the porous and fluid layer, respectively.

Under the steady state condition, we seek the form in fluid and porous layer as

$$[u, v, w, P, T, \vec{H}] = [0, 0, 0, P_b(z), T_b(z), H_0(z)] \tag{11}$$

$$[u_m, v_m, w_m, P_m, T_m, \vec{H}] = [0, 0, 0, P_{mb}(z_m), T_{mb}(z_m), H_0(z_m)] \tag{12}$$

The temperature distributions $T_b(z)$ and $T_{mb}(z_m)$ are found to be

$$T_b(z) = \frac{-Qz(z-d)}{2\kappa} + \frac{(T_u - T_0)h(z)}{d} + T_0 \quad 0 \leq z \leq d \tag{13}$$

$$T_{mb}(z_m) = \frac{-Q_m z_m(z_m + d_m)}{2\kappa_m} + \frac{(T_0 - T_l)h_m(z_m)}{d_m} + T_0 \quad -d_m \leq z_m \leq 0 \tag{14}$$

where $T_0 = \frac{\kappa d_m T_u + \kappa_m d T_l}{\kappa d_m + \kappa_m d} + \frac{d d_m (Q_m d_m + Q d)}{2(\kappa d_m + \kappa_m d)}$ is the interface temperature at $z = z_m = 0$ and $h(z)$ and $h_m(z_m)$ are the non-dimensional temperature gradients with $\int_0^1 h(z)dz = 1$ and $\int_0^1 h_m(z_m)dz_m = 1$ in fluid and porous layer respectively and subscript 'b' denote the basic state.

We superimpose infinitesimal disturbances on the basic state for fluid and porous layer, respectively

$$[\vec{q}, P, T, \vec{H}] = [0, P_b(z), T_b(z), H_0(z)] + [\vec{q}', P', \theta, \vec{H}'] \tag{15}$$

$$[\vec{q}_m, P_m, T_m, \vec{H}] = [0, P_{mb}(z_m), T_{mb}(z_m), H_0(z_m)] + [\vec{q}'_m, P'_m, \theta_m, \vec{H}'] \tag{16}$$

where the primed quantities are the perturbed ones over their equilibrium counterparts. Now introducing (15) and (16) are substituted into the (1) to (10) and are linearized in the usual manner. Next, the pressure term is eliminated from (3) and (8) by taking curl twice on these two equations and only the vertical component is

retained. The variables are then non- dimensionalized using d, $\dfrac{d^2}{\kappa}$, $\dfrac{\kappa}{d}$, $T_0 - T_u$ and H_0 as the units of length, time, velocity, temperature and the magnetic field in the fluid layer and d_m, $\dfrac{d_m^2}{\kappa_m}$, $\dfrac{\kappa_m}{d_m}$, $T_l - T_0$ as the corresponding characteristic quantities in the porous layer.

The dimensionless equations (after neglecting the primes) are:

$$\frac{1}{\Pr}\frac{\partial \nabla^2 w}{\partial t} = \nabla^4 w + Q\tau_{fm}\frac{\partial \nabla^2 H_z}{\partial z} \tag{17}$$

$$\frac{\partial \theta}{\partial t} = \nabla^2 \theta + w h(z) + R_I \frac{(2z-1)w}{2(T_0 - T_u)} \tag{18}$$

$$\frac{\partial H_z}{\partial t} = \frac{\partial w}{\partial z} + \tau_{fm}\nabla^2 H_z \tag{19}$$

$$\frac{\beta^2}{\Pr_m}\frac{\partial \nabla_m^2 w_m}{\partial t} = \hat{\mu}\beta^2 \nabla_m^4 w_m - \nabla_m^2 w_m + \beta^2 Q_m \tau_{mm}\frac{\partial \nabla_m^2 H_{zm}}{\partial z_m} \tag{20}$$

$$A\frac{\partial \theta_m}{\partial t} = w_m h_m(z_m) + \nabla_m^2 \theta_m + R_{Im}\frac{(2z_m+1)w_m}{2(T_l - T_0)} \tag{21}$$

$$\varepsilon \frac{\partial H_{zm}}{\partial t} = \frac{\partial w_m}{\partial z} + \tau_{mm}\nabla_m^2 H_{zm} \tag{22}$$

where, for fluid layer, $\Pr = \dfrac{\nu}{\kappa}$, $Q = \dfrac{\mu_p H_0^2 d^2}{\mu\kappa\tau_{fm}}$, $\tau_{fm} = \dfrac{\nu_{mv}}{\kappa}$, $R_I = \dfrac{R_i}{d(T_0 - T_u)}$ are namely, the Prandtl number, the Chandrasekhar number, the diffusivity ratio and the internal Rayleigh number respectively. For the porous layer, $\Pr_m = \dfrac{\varepsilon\nu_m}{\kappa_m}$, $\beta^2 = \dfrac{K}{d_m^2} = Da$, β,

$\hat{\mu} = \dfrac{\mu_m}{\mu}$, $Q_m = \dfrac{\mu_p H_0^2 d_m^2}{\mu\kappa_m\tau_{mm}} = Q\varepsilon\hat{d}^2$, $\tau_{mm} = \dfrac{\nu_{em}}{\kappa_m}$, $R_{Im} = \dfrac{R_{im}}{d_m(T_l - T_0)}$ are namely, the Prandtl number, the Darcy number, the porous parameter, the viscosity ratio, the Chandrasekhar number, the diffusivity ratio of fluid in porous layer and the internal Rayleigh number respectively with $R_i = \dfrac{\phi d^2}{\kappa}$ and $R_{im} = \dfrac{\phi_m d_m^2}{\kappa_m}$.

Introducing the normal mode expansion procedure for both layers in the form

$$\begin{bmatrix} w \\ \theta \\ H \end{bmatrix} = \begin{bmatrix} W(z) \\ \Theta(z) \\ H(z) \end{bmatrix} f(x,y)e^{nt} \tag{23}$$

$$\begin{bmatrix} w_m \\ \theta_m \\ H \end{bmatrix} = \begin{bmatrix} W_m(z_m) \\ \Theta_m(z_m) \\ H(z_m) \end{bmatrix} f(x_m,y_m)e^{n_m t} \tag{24}$$

with $\nabla_2^2 f + a^2 f = 0$ and $\nabla_{2m}^2 f_m + a_m^2 f_m = 0$, where a and a_m are the non-dimensional horizontal wave numbers, n and n_m are the frequencies. Since the dimensional horizontal wave numbers must be

the same for the fluid and porous layers, we must have $\dfrac{a}{d} = \dfrac{a_m}{d_m}$ and hence $a_m = \hat{d}a$ where $\hat{d} = \dfrac{d_m}{d}$ is the depth ratio, $W(z)$ and $W_m(z_m)$ are the dimensionless vertical velocities in fluid and porous layer, respectively, $\Theta(z)$ and $\Theta_m(z_m)$ are the temperature distributions in fluid and porous layers, respectively.

Introducing (23) & (24) into the (17) to (22) and obtained for $0 \le z \le 1$ and $-1 \le z_m \le 0$, respectively

$$\left(D^2 - a^2 + \frac{n}{\Pr}\right)(D^2 - a^2)W = -Q\tau_{fm}D(D^2 - a^2)H \tag{25}$$

$$\left(D^2 - a^2 + n\right)\Theta(z) + \left[h(z) + R_I^*(2z-1)\right]W(z) = 0 \tag{26}$$

$$\left[\tau_{fm}\left(D^2 - a^2\right) + n\right]H + DW = 0 \tag{27}$$

$$[(D_m^2 - a_m^2)\hat{\mu}\beta^2 + \frac{n_m\beta^2}{\Pr_m} - 1](D_m^2 - a_m^2)W_m = \\ -Q_m\tau_{mm}\beta^2 D_m(D_m^2 - a_m^2)H(z_m) \tag{28}$$

$$\left(D_m{}^2 - a_m{}^2 + An_m\right)\Theta_m(z_m) \\ + \left[h_m(z_m) + R_{Im}^*(2z_m + 1)\right]W_m(z_m) = 0 \tag{29}$$

$$\left[\tau_{mm}\left(D_m^2 - a_m^2\right) + n_m\varepsilon\right]H(z_m) + DW_m = 0 \tag{30}$$

where $R_I^* = \dfrac{R_I}{2(T_0 - T_u)}$ and $R_{Im}^* = \dfrac{R_{Im}}{2(T_l - T_0)}$.

We assume that the principle of exchange stability to be valid for present problem, so we take $n = n_m = 0$ and eliminating the magnetic field in equations (25) and (28) using equations (27) and (30), we get in $0 \le z \le 1$ and $-1 \le z_m \le 0$, respectively.

$$\left(D^2 - a^2\right)^2 W(z) = QD^2W(z) \tag{31}$$

$$\left(D^2 - a^2\right)\Theta(z) + [h(z) + R_I^*(2z-1)]W(z) = 0 \tag{32}$$

$$\left[\left(D_m^2 - a_m^2\right)\hat{\mu}\beta^2 - 1\right]\left(D_m^2 - a_m^2\right)W_m(z_m) = \beta^2 Q_m D_m^2 W_m(z_m) \tag{33}$$

$$\left(D_m{}^2 - a_m{}^2\right)\Theta_m(z_m) + [h_m(z_m) + R_{Im}^*(2z_m + 1)]W_m(z_m) = 0 \tag{34}$$

Boundary conditions

The boundary conditions are non-dimensionalized and then subjected to normal mode expansion and are

$D^2 W(1) + M a^2 \Theta(1) = 0$,
$W(1) = 0$, $W_m(-1) = 0$, $D_m W_m(-1) = 0$,
$\hat{T}W(0) = W_m(0)$, $\hat{T}\hat{d}DW(0) = D_m W_m(0)$,
$\hat{T}\hat{d}^2\left(D^2 + a^2\right)W(0) = \left(D_m^2 + a_m^2\right)W_m(0)$,
$\hat{T}\hat{d}^3\beta^2\left(D^3 W(0) - 3a^2 DW(0)\right) = -D_m W_m(0) \\ \qquad\qquad + \hat{\mu}\beta^2\left(D_m^3 W_m(0) - 3a_m^2 D_m W_m(0)\right)$
$D\Theta(1) = 0$, $\Theta(0) = \hat{T}\Theta_m(0)$, $D\Theta(0) = D_m\Theta_m(0)$, $\Theta_m(-1) = 0$ $\qquad$ (35)

where $\hat{T} = \dfrac{T_l - T_0}{T_0 - T_u}$ is the thermal ratio and

$M = -\dfrac{\partial \sigma_t}{\partial T} \dfrac{(T_0 - T_u)d}{\mu \kappa}$ is the thermal Marangoni number.

Method of solution

The resulting eigenvalue problem solved exactly, the vertical velocities for fluid and porous layer $W(z)$ and $W_m(z_m)$ are found using the velocity boundary conditions (35),

$$W(z) = A_1 \left[\cosh \delta z + a_1 \sinh \delta z + a_2 \cosh \zeta z + a_3 \sinh \zeta z \right] \qquad (36)$$

$$W_m(z_m) = A_1 \begin{bmatrix} a_4 \cosh \eta_m z_m + a_5 \sinh \eta_m z_m + a_6 \cosh \psi_m z_m \\ + a_7 \sinh \psi_m z_m \end{bmatrix} \qquad (37)$$

where

$$\delta = \sqrt{\dfrac{\sqrt{Q} + \sqrt{Q + 4a^2}}{2}}, \quad \zeta = \sqrt{\dfrac{\sqrt{Q} - \sqrt{Q + 4a^2}}{2}}$$

$$\eta_m = \sqrt{\dfrac{E + \sqrt{E^2 - 4F}}{2}}, \quad \psi_m = \sqrt{\dfrac{E - \sqrt{E^2 - 4F}}{2}},$$

$$E = \dfrac{2\hat{\mu}\beta^2 a_m^2 + 1 + Q_m \beta^2}{\hat{\mu}\beta^2}, \quad F = \dfrac{\hat{\mu}\beta^2 a_m^4 + a_m^2}{\hat{\mu}\beta^2},$$

$$a_1 = \dfrac{-(a_6 \delta_{15} + a_7 \delta_{16} + \delta_{17})}{\delta_{14}}, \quad a_2 = a_6 \delta_5 + \delta_6, \quad a_3 = \dfrac{(a_1 \delta_{10} + a_7 \delta_{11})}{\delta_9},$$

$$a_4 = a_6 \delta_8 + \delta_7, \quad a_5 = a_1 \delta_{12} + a_7 \delta_{13}, \quad a_6 = \dfrac{\delta_{23}\delta_{25} - \delta_{26}\delta_{22}}{\delta_{25}\delta_{21} - \delta_{24}\delta_{22}},$$

$$a_7 = \dfrac{\delta_{23}\delta_{24} - \delta_{26}\delta_{21}}{\delta_{24}\delta_{22} - \delta_{25}\delta_{21}}, \quad \delta_1 = \hat{T}\beta^2 \hat{d}^3 (\delta^3 - 3a^2 \delta),$$

$$\delta_2 = \hat{T}\beta^2 \hat{d}^3 (\zeta^3 - 3a^2 \zeta), \quad \delta_3 = \hat{\mu}\beta^2(\eta_m^3 - 3a_m^2 \eta_m) - \eta_m,$$

$$\delta_4 = \hat{\mu}\beta^2 (\psi_m^3 - 3a_m^2 \psi_m) - \psi_m, \quad \delta_5 = \dfrac{\hat{\mu}[(\psi_m^2 + a_m^2) - \hat{T}(\eta_m^2 + a_m^2)]}{\hat{T}\hat{d}^2(\zeta^2 + a^2) - \hat{\mu}\hat{T}(\eta_m^2 + a_m^2)},$$

$$\delta_6 = \dfrac{\hat{\mu}(\eta_m^2 + a_m^2) - (\delta^2 + a^2)]}{\hat{d}^2(\zeta^2 + a^2) - \hat{\mu}(\eta_m^2 + a_m^2)}, \quad \delta_7 = \hat{T}(1 + \delta_6), \quad \delta_8 = \hat{T}\delta_5 - 1,$$

$$\delta_9 = \delta_2 - \dfrac{\hat{T}\hat{d}\zeta\delta_3}{\eta_m}, \quad \delta_{10} = -\delta_1 + \dfrac{\hat{T}\hat{d}\delta\delta_3}{\eta_m}, \quad \delta_{11} = \delta_4 - \dfrac{\psi_m \delta_3}{\eta_m},$$

$$\delta_{12} = \dfrac{1}{\eta_m}\left(\hat{T}\hat{d}\delta + \dfrac{\zeta\delta_{10}}{\delta_9} \right), \quad \delta_{13} = \dfrac{1}{\eta_m}\left(\dfrac{\hat{T}\hat{d}\zeta\delta_{11}}{\delta_9} - \psi_m \right),$$

$$\delta_{14} = \sinh \delta + \dfrac{\delta_{10}}{\delta_9} \sinh \zeta, \quad \delta_{15} = \delta_5 \cosh \zeta, \quad \delta_{16} = \dfrac{\delta_{11}\sinh \zeta}{\delta_9},$$

$$\delta_{17} = \delta_6 \cosh \zeta + \cosh \delta, \quad \delta_{18} = \dfrac{\delta_{12}\delta_{15}}{\delta_{14}}, \quad \delta_{19} = \dfrac{\delta_{12}\delta_{16}}{\delta_{14}} + \delta_{13}, \quad \delta_{20} = \dfrac{\delta_{12}\delta_{17}}{\delta_{14}}$$

$$\delta_{21} = \delta_8 \cosh \eta_m - \delta_{18} \sinh \eta_m + \cosh \psi_m, \quad \delta_{22} = -\delta_{19} \sinh \eta_m - \sinh \psi_m,$$

$$\delta_{23} = \delta_{20} \sinh \eta_m - \delta_7 \cosh \eta_m,$$

$$\delta_{24} = -\eta_m \delta_8 \sinh \eta_m - \delta_{18}\eta_m \cosh \eta_m - \psi_m \sinh \psi_m,$$

$$\delta_{25} = -\eta_m \delta_{19} \cosh \eta_m + \psi_m \cosh \psi_m, \quad \delta_{26} = \eta_m \delta_7 \sinh \eta_m + \delta_{20}\eta_m \cosh \eta_m$$

Linear Temperature Profile

For linear temperature profile,

$$h(z) = 1 \text{ and } h_m(z_m) = 1 \qquad (38)$$

Introducing (38) into (32) & (34), using the temperature boundary conditions, we get $\Theta(z)$ and $\Theta_m(z_m)$ as

$$\Theta(z) = A_1 \left[c_1 \cosh az + c_2 \sinh az + g_1(z) \right] \qquad (39)$$

$$\Theta_m(z_m) = A_1 \left[c_3 \cosh a_m z_m + c_4 \sinh a_m z_m + g_{1m}(z_m) \right] \qquad (40)$$

where $g_1(z) = A_1[\delta_{27} - \delta_{28} + \delta_{29} - \delta_{30}]$,

$g_{1m}(z_m) = A_1[\delta_{31} - \delta_{32} + \delta_{33} - \delta_{34}]$,

$$\delta_{27} = \dfrac{E_1 + E_2 z}{(\delta^2 - a^2)}(\cosh \delta z + a_1 \sinh \delta z),$$

$$\delta_{28} = \dfrac{2\delta E_2}{(\delta^2 - a^2)^2}(a_1 \cosh \delta z + \sinh \delta z),$$

$$\delta_{29} = \dfrac{E_1 + E_2 z}{(\zeta^2 - a^2)}(a_2 \cosh \zeta z + a_3 \sinh \zeta z),$$

$$\delta_{30} = \dfrac{2\zeta E_2}{(\zeta^2 - a^2)^2}(a_3 \cosh \zeta z + a_2 \sinh \zeta z),$$

$$\delta_{31} = \dfrac{E_{1m} + E_{2m} z_m}{(\eta_m^2 - a_m^2)}(a_4 \cosh \eta_m z_m + a_5 \sinh \eta_m z_m),$$

$$\delta_{32} = \dfrac{2E_{2m}\eta_m}{(\eta_m^2 - a_m^2)^2}(a_5 \cosh \eta_m z_m + a_4 \sinh \eta_m z_m),$$

$$\delta_{33} = \dfrac{E_{1m} + E_{2m} z_m}{(\psi_m^2 - a_m^2)}(a_6 \cosh \psi_m z_m + a_7 \sinh \psi_m z_m),$$

$$\delta_{34} = \dfrac{2E_{2m}\psi_m}{(\psi_m^2 - a_m^2)^2}(a_7 \cosh \psi_m z_m + a_6 \sinh \psi_m z_m),$$

$E_1 = R_I^* - 1, \quad E_2 = -2R_I^*, \quad E_{1m} = -R_{Im}^* - 1, \quad E_{2m} = -2R_{Im}^*$,

$c_1 = \hat{T}c_3 + \Delta_2 - \Delta_3, \quad c_2 = \dfrac{1}{a}(c_4 a_m + \Delta_4 - \Delta_5)$,

$c_3 = \dfrac{\Delta_8 \Delta_{10} + \Delta_{11}\Delta_7}{\Delta_6 \Delta_{10} + \Delta_9 \Delta_7}, \quad c_4 = \dfrac{\Delta_8 \Delta_9 - \Delta_{11}\Delta_6}{-\Delta_7 \Delta_9 - \Delta_{10}\Delta_6}$,

$\Delta_1 = -[\delta_{35} + \delta_{36} + \delta_{37} + \delta_{38}]$,

$$\delta_{35} = \dfrac{(E_1 + E_2)\delta}{(\delta^2 - a^2)}(a_1 \cosh \delta + \sinh \delta),$$

$$\delta_{36} = \left(\dfrac{E_2}{(\delta^2 - a^2)} - \dfrac{2\delta^2 E_2}{(\delta^2 - a^2)^2} \right)(\cosh \delta + a_1 \sinh \delta),$$

$$\delta_{37} = \dfrac{(E_1 + E_2)\zeta}{(\zeta^2 - a^2)}(a_3 \cosh \zeta + a_2 \sinh \zeta),$$

$$\delta_{38} = \left(\dfrac{E_2}{(\zeta^2 - a^2)} - \dfrac{2\zeta^2 E_2}{(\zeta^2 - a^2)^2} \right)(a_2 \cosh \zeta + a_3 \sinh \zeta),$$

$$\Delta_2 = \hat{T}\left[\dfrac{E_{1m}a_4}{(\eta_m^2 - a_m^2)} - \dfrac{2E_{2m}\eta_m a_5}{(\eta_m^2 - a_m^2)^2} + \dfrac{E_{1m}a_6}{(\psi_m^2 - a_m^2)} - \dfrac{2E_{2m}\psi_m a_7}{(\psi_m^2 - a_m^2)^2} \right],$$

$$\Delta_3 = \dfrac{E_1}{(\delta^2 - a^2)} - \dfrac{2\delta a_1 E_2}{(\delta^2 - a^2)^2} + \dfrac{a_2 E_1}{(\zeta^2 - a^2)} - \dfrac{2\zeta E_2 a_3}{(\zeta^2 - a^2)^2},$$

$$\Delta_4 = \dfrac{E_{2m}a_4}{(\eta_m^2 - a_m^2)} + \dfrac{E_{1m}a_5 \eta_m}{(\eta_m^2 - a_m^2)} - \dfrac{2\eta_m^2 E_{2m}a_4}{(\eta_m^2 - a_m^2)^2} + \Delta_{400},$$

$$\Delta_{400} = \dfrac{E_{2m}a_6}{(\psi_m^2 - a_m^2)} + \dfrac{E_{1m}a_7 \psi_m}{(\psi_m^2 - a_m^2)} - \dfrac{2\psi_m^2 E_{2m}a_6}{(\psi_m^2 - a_m^2)^2},$$

$$\Delta_5 = \dfrac{E_1 \delta a_1 + E_2}{(\delta^2 - a^2)} - \dfrac{2E_2 \delta^2}{(\delta^2 - a^2)^2} + \dfrac{E_1 \zeta a_3 + a_2 E_2}{(\zeta^2 - a^2)} - \dfrac{2E_2 \zeta^2 a_2}{(\zeta^2 - a^2)^2},$$

$\Delta_6 = \cosh a_m, \quad \Delta_7 = \sinh a_m, \quad \Delta_8 = -[\delta_{39} - \delta_{40} + \delta_{41} - \delta_{42}]$,

$$\delta_{39} = \dfrac{E_{1m} - E_{2m}}{(\eta_m^2 - a_m^2)}(a_4 \cosh \eta_m - a_5 \sinh \eta_m),$$

$$\delta_{40} = \dfrac{2E_{2m}\eta_m}{(\eta_m^2 - a_m^2)^2}(a_5 \cosh \eta_m - a_4 \sinh \eta_m),$$

$$\delta_{41} = \dfrac{E_{1m} - E_{2m}}{(\psi_m^2 - a_m^2)}(a_6 \cosh \psi_m - a_7 \sinh \psi_m),$$

$$\delta_{42} = \dfrac{2E_{2m}\psi_m}{(\psi_m^2 - a_m^2)^2}(a_7 \cosh \psi_m - a_6 \sinh \psi_m),$$

$\Delta_9 = \hat{T}a\sin ha$, $\Delta_{10} = a_m\cosh a$,

$\Delta_{11} = \Delta_1 - (\Delta_2 - \Delta_3)a\sinh a - (\Delta_4 - \Delta_5)\cosh a$

The thermal Marangoni number for this model from (35) as follows

$$M_1 = \frac{-[\delta^2(\cosh\delta z + a_1\sinh\delta z) + \zeta^2(a_2\cosh\zeta z + a_3\sinh\zeta z)]}{a^2(c_1\cosh a + c_2\sinh a + \Lambda_1 + \Lambda_2)} \quad (41)$$

where

$$\Lambda_1 = \frac{E_1 + E_2}{(\delta^2 - a^2)}(\cosh\delta + a_1\sinh\delta) - \frac{2\delta E_2}{(\delta^2 - a^2)^2}(a_1\cosh\delta + \sinh\delta)$$

$$\Lambda_2 = \frac{E_1 + E_2}{(\zeta^2 - a^2)}(a_2\cosh\zeta + a_3\sinh\zeta) - \frac{2\zeta E_2}{(\zeta^2 - a^2)^2}(a_3\cosh\zeta + a_2\sinh\zeta)$$

Parabolic temperature profile

For parabolic temperature profile,

$$h(z) = 2z \text{ and } h_m(z_m) = 2z_m \quad (42)$$

Introducing (42) into (32) & (34), using the temperature boundary conditions, we get $\Theta(z)$ and $\Theta_m(z_m)$ as

$$\Theta(z) = A_1[c_5\cosh az + c_6\sinh az + g_2(z)] \quad (43)$$

$$\Theta_m(z_m) = A_1[c_7\cosh a_m z_m + c_8\sinh a_m z_m + g_{2m}(z_m)] \quad (44)$$

where $g_2(z) = A_1[\delta_{43} - \delta_{44} + \delta_{45} - \delta_{46}]$,

$g_{2m}(z_m) = A_1[\delta_{47} - \delta_{48} + \delta_{49} - \delta_{50}]$,

$\delta_{43} = \frac{E_3 + E_4 z}{(\delta^2 - a^2)}(\cosh\delta z + a_1\sinh\delta z)$,

$\delta_{44} = \frac{2\delta E_4}{(\delta^2 - a^2)^2}(a_1\cosh\delta z + \sinh\delta z)$,

$\delta_{45} = \frac{E_3 + E_4 z}{(\zeta^2 - a^2)}(a_2\cosh\zeta z + a_3\sinh\zeta z)$,

$\delta_{46} = \frac{2\zeta E_4}{(\zeta^2 - a^2)^2}(a_3\cosh\zeta z + a_2\sinh\zeta z)$,

$\delta_{47} = \frac{E_{3m} + E_{4m}z_m}{(\eta_m^2 - a_m^2)}(a_4\cosh\eta_m z_m + a_5\sinh\eta_m z_m)$,

$\delta_{48} = \frac{2E_{4m}\eta_m}{(\eta_m^2 - a_m^2)^2}(a_5\cosh\eta_m z_m + a_4\sinh\eta_m z_m)$,

$\delta_{49} = \frac{E_{3m} + E_{4m}z_m}{(\psi_m^2 - a_m^2)}(a_6\cosh\psi_m z_m + a_7\sinh\psi_m z_m)$,

$\delta_{50} = \frac{2E_{4m}\psi_m}{(\psi_m^2 - a_m^2)^2}(a_7\cosh\psi_m z_m + a_6\sinh\psi_m z_m)$,

$E_3 = R_l^*$, $E_4 = -2(1 + R_l^*)$, $E_{3m} = -R_{lm}^* - 1$, $E_{4m} = -2(1 + R_{lm}^*)$,

$c_5 = \hat{T}c_7 + \Delta_{13} - \Delta_{14}$, $c_6 = \frac{1}{a}(c_8 a_m + \Delta_{15} - \Delta_{16})$, $c_7 = \frac{\Delta_{19}\Delta_{21} + \Delta_{22}\Delta_{18}}{\Delta_{17}\Delta_{21} + \Delta_{20}\Delta_{18}}$,

$c_8 = \frac{\Delta_{20}\Delta_{19} - \Delta_{22}\Delta_{17}}{-\Delta_{18}\Delta_{20} - \Delta_{21}\Delta_{17}}$, $\Delta_{12} = -[\delta_{51} + \delta_{52} + \delta_{53} + \delta_{54}]$,

$\delta_{51} = \frac{(E_3 + E_4)\delta}{(\delta^2 - a^2)}(a_1\cosh\delta + \sinh\delta)$

$\delta_{52} = \left(\frac{E_4}{(\delta^2 - a^2)} - \frac{2\delta^2 E_4}{(\delta^2 - a^2)^2}\right)(\cosh\delta + a_1\sinh\delta)$,

$\delta_{53} = \frac{(E_3 + E_4)\zeta}{(\zeta^2 - a^2)}(a_3\cosh\zeta + a_2\sinh\zeta)$,

$\delta_{54} = \left(\frac{E_4}{(\zeta^2 - a^2)} - \frac{2\zeta^2 E_4}{(\zeta^2 - a^2)^2}\right)(a_2\cosh\zeta + a_3\sinh\zeta)$,

$\Delta_{13} = \hat{T}\left[\frac{E_{3m}a_4}{(\eta_m^2 - a_m^2)} - \frac{2E_{4m}\eta_m a_5}{(\eta_m^2 - a_m^2)^2} + \frac{E_{3m}a_6}{(\psi_m^2 - a_m^2)} - \frac{2E_{4m}\psi_m a_7}{(\psi_m^2 - a_m^2)^2}\right]$,

$\Delta_{14} = \frac{E_3}{(\delta^2 - a^2)} - \frac{2\delta a_1 E_4}{(\delta^2 - a^2)^2} + \frac{a_2 E_3}{(\zeta^2 - a^2)} - \frac{2\zeta E_4 a_3}{(\zeta^2 - a^2)^2}$,

$\Delta_{15} = \frac{E_{4m}a_4}{(\eta_m^2 - a_m^2)} + \frac{E_{3m}a_5\eta_m}{(\eta_m^2 - a_m^2)} - \frac{2\eta_m^2 E_{4m}a_4}{(\eta_m^2 - a_m^2)^2} + \Delta_{150}$,

$\Delta_{150} = \frac{E_{4m}a_6}{(\psi_m^2 - a_m^2)} + \frac{E_{3m}a_7\psi_m}{(\psi_m^2 - a_m^2)} - \frac{2\psi_m^2 E_{4m}a_6}{(\psi_m^2 - a_m^2)^2}$,

$\Delta_{16} = \frac{E_3\delta a_1 + E_4}{(\delta^2 - a^2)} - \frac{2E_4\delta^2}{(\delta^2 - a^2)^2} + \frac{E_3\zeta a_3 + a_2 E_4}{(\zeta^2 - a^2)} - \frac{2E_4\zeta^2 a_2}{(\zeta^2 - a^2)^2}$,

$\Delta_{17} = \cosh a_m$, $\Delta_{18} = \sinh a_m$, $\Delta_{19} = -[\delta_{55} - \delta_{56} + \delta_{57} - \delta_{58}]$,

$\delta_{55} = \frac{E_{3m} - E_{4m}}{(\eta_m^2 - a_m^2)}(a_4\cosh\eta_m - a_5\sinh\eta_m)$,

$\delta_{56} = \frac{2E_{4m}\eta_m}{(\eta_m^2 - a_m^2)^2}(a_5\cosh\eta_m - a_4\sinh\eta_m)$,

$\delta_{57} = \frac{E_{3m} - E_{4m}}{(\psi_m^2 - a_m^2)}(a_6\cosh\psi_m - a_7\sinh\psi_m)$,

$\delta_{58} = \frac{2E_{4m}\psi_m}{(\psi_m^2 - a_m^2)^2}(a_7\cosh\psi_m - a_6\sinh\psi_m)$,

$\Delta_{20} = \hat{T}a\sin ha$, $\Delta_{21} = a_m\cosh a$,

$\Delta_{22} = \Delta_{12} - (\Delta_{13} - \Delta_{14})a\sinh a - (\Delta_{15} - \Delta_{16})\cosh a$

The thermal Marangoni number for this model from (35) as follows

$$M_2 = \frac{-[\delta^2(\cosh\delta z + a_1\sinh\delta z) + \zeta^2(a_2\cosh\zeta z + a_3\sinh\zeta z)]}{a^2(c_5\cosh a + c_6\sinh a + \Lambda_3 + \Lambda_4)}$$
(45)

$$\Lambda_3 = \frac{E_3 + E_4}{(\delta^2 - a^2)}(\cosh\delta + a_1\sinh\delta) - \frac{2\delta E_4}{(\delta^2 - a^2)^2}(a_1\cosh\delta + \sinh\delta)$$

$$\Lambda_4 = \frac{E_3 + E_4}{(\zeta^2 - a^2)}(a_2\cosh\zeta + a_3\sinh\zeta) - \frac{2\zeta E_4}{(\zeta^2 - a^2)^2}(a_3\cosh\zeta + a_2\sinh\zeta)$$

Inverted parabolic temperature profile

For inverted parabolic temperature profile,

$$h(z) = 2(1 - z) \text{ and } h_m(z_m) = 2(1 - z_m) \quad (46)$$

Introducing (46) into (32) & (34), using the temperature boundary conditions, we get $\Theta(z)$ and $\Theta_m(z_m)$ as

$$\Theta(z) = A_1[c_9\cosh az + c_{10}\sinh az + g_3(z)] \quad (47)$$

$$\Theta_m(z_m) = A_1[c_{11}\cosh a_m z_m + c_{12}\sinh a_m z_m + g_{3m}(z_m)] \quad (48)$$

where $g_3(z) = A_1[\delta_{59} - \delta_{60} + \delta_{61} - \delta_{62}]$,

$g_{3m}(z_m) = A_1[\delta_{63} - \delta_{64} + \delta_{65} - \delta_{66}]$,

$\delta_{59} = \frac{E_5 + E_6 z}{(\delta^2 - a^2)}(\cosh\delta z + a_1\sinh\delta z)$,

$\delta_{60} = \frac{2\delta E_6}{(\delta^2 - a^2)^2}(a_1\cosh\delta z + \sinh\delta z)$,

$\delta_{61} = \frac{E_5 + E_6 z}{(\zeta^2 - a^2)}(a_2\cosh\zeta z + a_3\sinh\zeta z)$,

$$\delta_{62} = \frac{2\zeta E_6}{(\zeta^2 - a^2)^2}(a_3 \cosh \zeta z + a_2 \sinh \zeta z),$$

$$\delta_{63} = \frac{E_{5m} + E_{6m} z_m}{(\eta_m^2 - a_m^2)}(a_4 \cosh \eta_m z_m + a_5 \sinh \eta_m z_m),$$

$$\delta_{64} = \frac{2E_{6m} \eta_m}{(\eta_m^2 - a_m^2)^2}(a_5 \cosh \eta_m z_m + a_4 \sinh \eta_m z_m),$$

$$\delta_{65} = \frac{E_{5m} + E_{6m} z_m}{(\psi_m^2 - a_m^2)}(a_6 \cosh \psi_m z_m + a_7 \sinh \psi_m z_m),$$

$$\delta_{66} = \frac{2E_{6m} \psi_m}{(\psi_m^2 - a_m^2)^2}(a_7 \cosh \psi_m z_m + a_6 \sinh \psi_m z_m),$$

$$E_5 = R_I^* - 2, \ E_6 = 2 - 2R_I^*, \ E_{5m} = -2 - R_{Im}^* - 1, \ E_{6m} = 2 - 2R_{Im}^*,$$

$$c_9 = \hat{T} c_{11} + \Delta_{24} - \Delta_{25}, \ c_{10} = \frac{1}{a}(c_{12} a_m + \Delta_{26} - \Delta_{27}),$$

$$c_{11} = \frac{\Delta_{30}\Delta_{32} + \Delta_{33}\Delta_{29}}{\Delta_{28}\Delta_{32} + \Delta_{29}\Delta_{31}}, \ c_{12} = \frac{\Delta_{30}\Delta_{31} - \Delta_{33}\Delta_{28}}{-\Delta_{31}\Delta_{29} - \Delta_{32}\Delta_{28}},$$

$$\Delta_{23} = -[\delta_{67} + \delta_{68} + \delta_{69} + \delta_{70}],$$

$$\delta_{67} = \frac{(E_5 + E_6)\delta}{(\delta^2 - a^2)}(a_1 \cosh \delta + \sinh \delta),$$

$$\delta_{68} = \left(\frac{E_6}{(\delta^2 - a^2)} - \frac{2\delta^2 E_6}{(\delta^2 - a^2)^2}\right)(\cosh \delta + a_1 \sinh \delta),$$

$$\delta_{69} = \frac{(E_5 + E_6)\zeta}{(\zeta^2 - a^2)}(a_3 \cosh \zeta + a_2 \sinh \zeta),$$

$$\delta_{70} = \left(\frac{E_6}{(\zeta^2 - a^2)} - \frac{2\zeta^2 E_6}{(\zeta^2 - a^2)^2}\right)(a_2 \cosh \zeta + a_3 \sinh \zeta),$$

$$\Delta_{24} = \hat{T}\left[\frac{E_{5m} a_4}{(\eta_m^2 - a_m^2)} - \frac{2E_{6m}\eta_m a_5}{(\eta_m^2 - a_m^2)^2} + \frac{E_{5m} a_6}{(\psi_m^2 - a_m^2)} - \frac{2E_{6m}\psi_m a_7}{(\psi_m^2 - a_m^2)^2}\right],$$

$$\Delta_{25} = \frac{E_5}{(\delta^2 - a^2)} - \frac{2\delta a_1 E_6}{(\delta^2 - a^2)^2} + \frac{a_2 E_5}{(\zeta^2 - a^2)} - \frac{2\zeta E_6 a_3}{(\zeta^2 - a^2)^2},$$

$$\Delta_{26} = \frac{E_{6m} a_4}{(\eta_m^2 - a_m^2)} + \frac{E_{5m} a_5 \eta_m}{(\eta_m^2 - a_m^2)} - \frac{2\eta_m^2 E_{6m} a_4}{(\eta_m^2 - a_m^2)^2} + \Delta_{260},$$

$$\Delta_{260} = \frac{E_{6m} a_6}{(\psi_m^2 - a_m^2)} + \frac{E_{5m} a_7 \psi_m}{(\psi_m^2 - a_m^2)} - \frac{2\psi_m^2 E_{6m} a_6}{(\psi_m^2 - a_m^2)^2},$$

$$\Delta_{27} = \frac{E_5 \delta a_1 + E_6}{(\delta^2 - a^2)} - \frac{2E_6 \delta^2}{(\delta^2 - a^2)^2} + \frac{E_5 \zeta a_3 + a_2 E_6}{(\zeta^2 - a^2)} - \frac{2E_6 \zeta^2 a_2}{(\zeta^2 - a^2)^2},$$

$$\Delta_{28} = \cosh a_m, \ \Delta_{29} = \sinh a_m, \ \Delta_{30} = -[\delta_{71} - \delta_{72} + \delta_{73} - \delta_{74}],$$

$$\delta_{71} = \frac{E_{5m} - E_{6m}}{(\eta_m^2 - a_m^2)}(a_4 \cosh \eta_m - a_5 \sinh \eta_m),$$

$$\delta_{72} = \frac{2E_{6m}\eta_m}{(\eta_m^2 - a_m^2)^2}(a_5 \cosh \eta_m - a_4 \sinh \eta_m),$$

$$\delta_{73} = \frac{E_{5m} - E_{6m}}{(\psi_m^2 - a_m^2)}(a_6 \cosh \psi_m - a_7 \sinh \psi_m),$$

$$\delta_{74} = \frac{2E_{6m}\psi_m}{(\psi_m^2 - a_m^2)^2}(a_7 \cosh \psi_m - a_6 \sinh \psi_m),$$

$$\Delta_{31} = \hat{T} a \sinh a, \ \Delta_{32} = a_m \cosh a,$$

$$\Delta_{33} = \Delta_{23} - (\Delta_{24} - \Delta_{25})a \sinh a - (\Delta_{26} - \Delta_{27})\cosh a$$

The thermal Marangoni number for this model from (35) as follows

$$M_3 = \frac{-[\delta^2(\cosh \delta z + a_1 \sinh \delta z) + \zeta^2(a_2 \cosh \zeta z + a_3 \sinh \zeta z)]}{a^2(c_9 \cosh a + c_{10} \sinh a + \Lambda_5 + \Lambda_6)} \quad (49)$$

$$\Lambda_5 = \frac{E_5 + E_6}{(\delta^2 - a^2)}(\cosh \delta + a_1 \sinh \delta) - \frac{2\delta E_6}{(\delta^2 - a^2)^2}(a_1 \cosh \delta + \sinh \delta)$$

$$\Lambda_6 = \frac{E_5 + E_6}{(\zeta^2 - a^2)}(a_2 \cosh \zeta + a_3 \sinh \zeta) - \frac{2\zeta E_6}{(\zeta^2 - a^2)^2}(a_3 \cosh \zeta + a_2 \sinh \zeta)$$

RESULTS AND DISCUSSION

The eigenvalue, thermal Marangoni number M for non-Darcian-Benard-magneto-surface tension driven convection is obtained as an expression of the diverse parameters, which are $\hat{d}$, a and a_m, β, $\hat{T}$, $\hat{\mu}$, R_I and R_{Im}, Q namely, the depth ratio, the horizontal wavenumbers, the porous parameter, the thermal ratio, viscosity ratio, the internal Rayleigh numbers for fluid and porous layers and the Chandrasekhar number respectively. The curves of thermal Marangoni number M are drawn as a function of the thermal ratio $\hat{T}$. By observing the graphs in Figures 2-6, it is evident that, for smaller values of $\hat{T}$, the thermal Marangoni number M falls till some value of $\hat{T}$, again thermal Marangoni rises as the value of thermal ratio rises. The weightage of the horizontal wave number a, the porous parameter β, the Chandrasekhar number Q, the viscosity ratio $\hat{\mu}$, the internal Rayleigh number R_I on non-Darcian-Benard-Magneto-Surface tension driven convection is explained in the upcoming graphs where with the variation of one parameter with the accompanying parameters are fixed as $Q = 10$, $\varepsilon = 1$, $\beta = 0.1$, $a = 2.5$, $\hat{d} = 2.5$, $\hat{\mu} = 2.5$, $R_I = -3$ and $R_{Im} = 1$.

Fig.2a-2c explain the variation of the horizontal wave number a on the value of thermal Marangoni number M for the values of $a = 1.5$, 2.0 and 2.5, for linear, parabolic and inverted parabolic temperature profiles respectively. From the curves, it is understandable that for smaller values of thermal ratio there is no much effect of this parameter on thermal Marangoni number. For larger values of thermal ratio, there is considerable effect of this parameter on thermal Marangoni number. For a fixed value of thermal ratio, the thermal Marangoni number reduces with an augment in the value of a. So, the system becomes firm for smaller values of the horizontal wave number. Analogous effects are seen for both uniform and non-uniform temperature profiles.

Fig.3a-3c discuss the importance of β, the porous parameter on the thermal Marangoni number and it is for $\beta = 1.1$, 1.2 and 1.3. The curves are diverging radically for all the temperature profiles, which means that the role of the porous parameter is most important for larger values of thermal ratio. For fixed value of thermal ratio, a boost in the value of β, boosts the Marangoni number. Hence, the system can be stabilized by boosting the value of β. Boosting the value of porous parameter is nothing but boosting permeability. Even though there is more permeability for the fluid in the porous layer, the system still tends to be stable which is quite interesting and may be due to influence of vertical magnetic field.

The role of Chandrasekhar number Q is discussed in Fig. 4a-4c for the three temperature profiles for values of $Q = 10$, 15 and 20. The hugely diverging curves for all the three profiles show the prominence of Q for larger thermal ratio values. For a fixed thermal ratio, an enhance in the value of Q, enhances the thermal Marangoni number, hence the non-Darcian-Benard-magneto-surface tension driven convection can be preponed by decreasing the value of Q and hence the system can be destabilized. This is physically reasonable as the application of magnetic field stabilizes non-Darcian-Benard-magneto-surface tension driven convection.
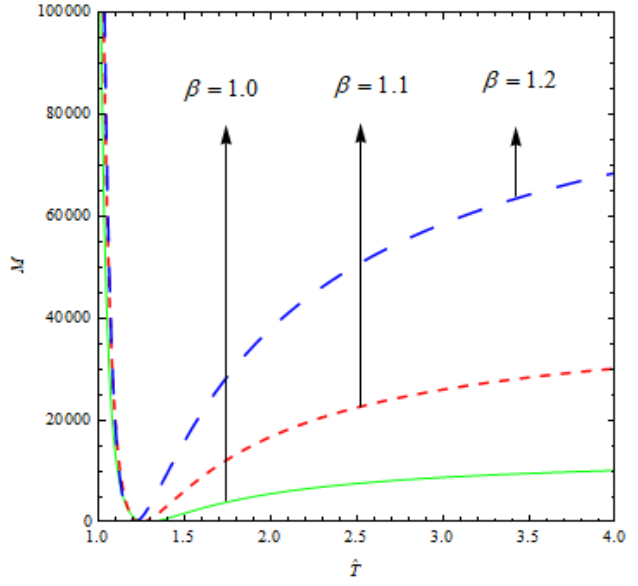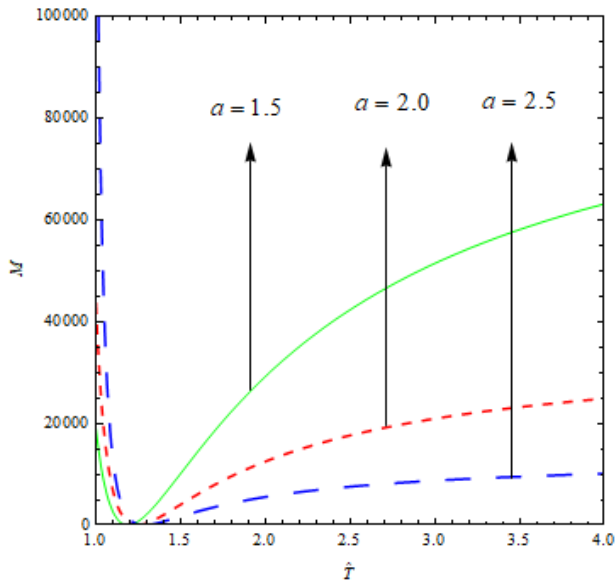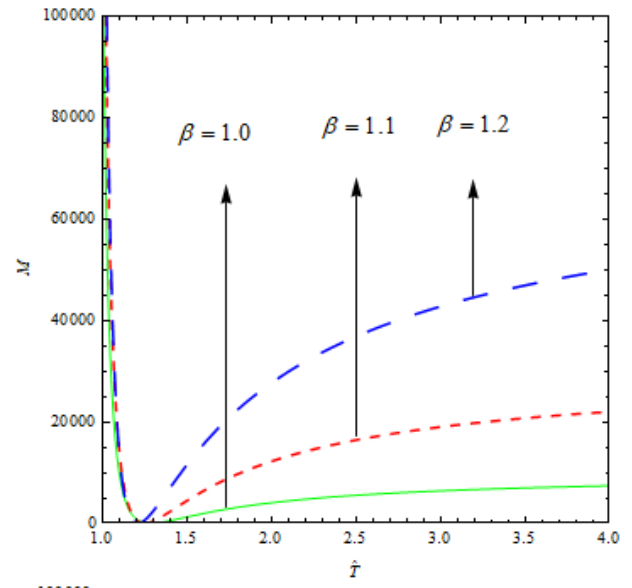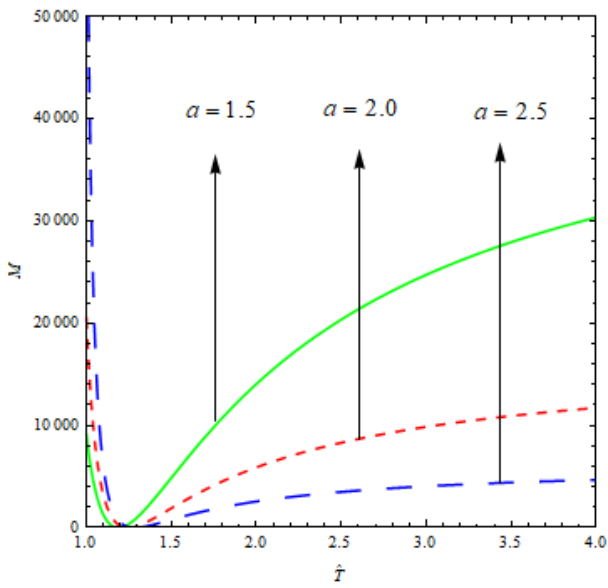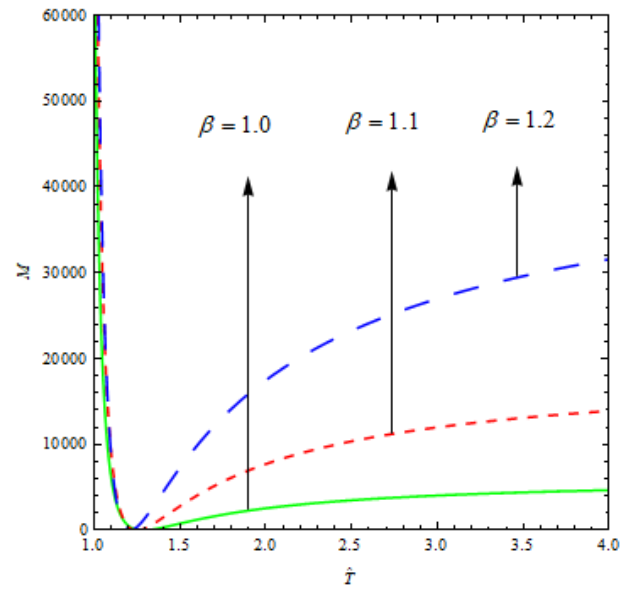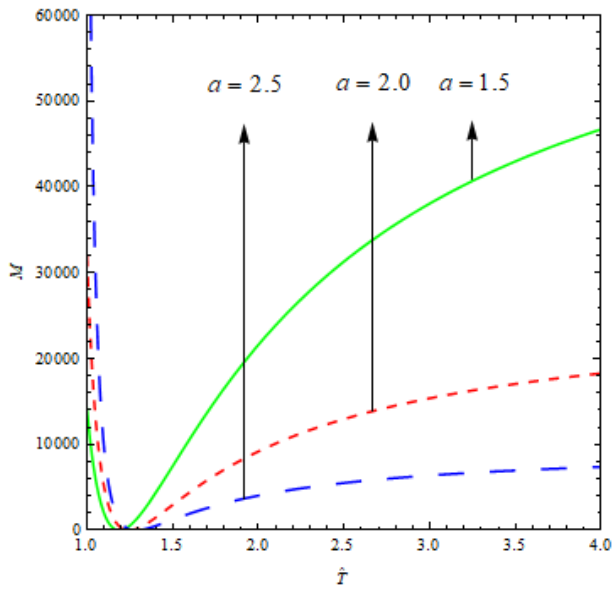
Fig. 2a-2c Thermal Marangoni number M versus thermal ratio $\hat{T}$ for different values of horizontal wave number a

Fig. 3a-3c Thermal Marangoni number M versus thermal ratio $\hat{T}$ for different values of porous parameter β
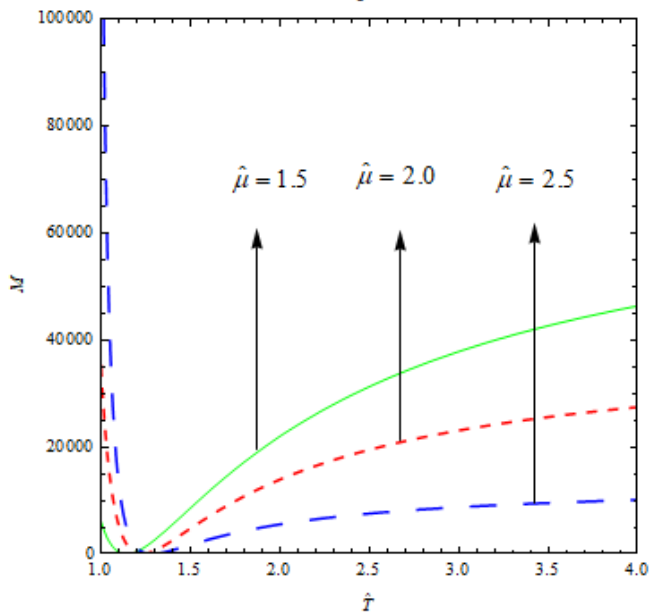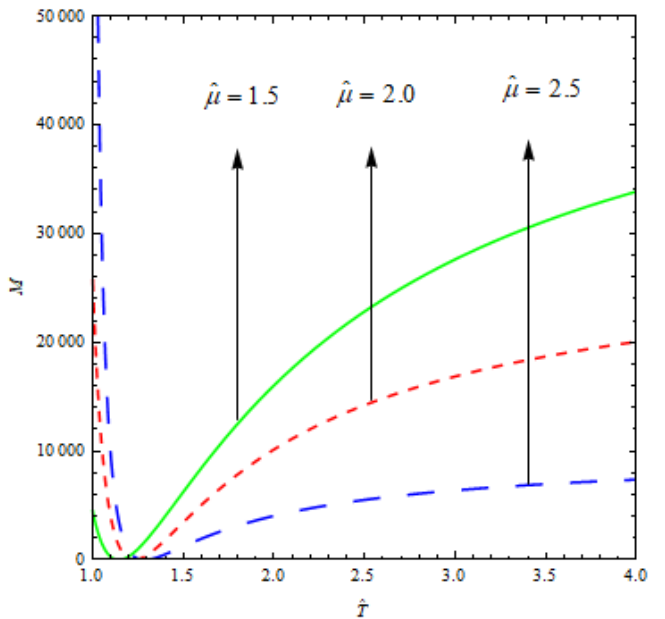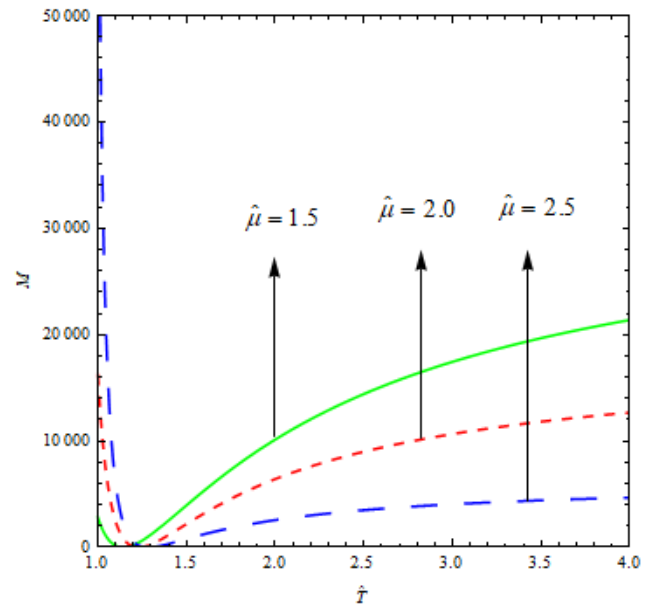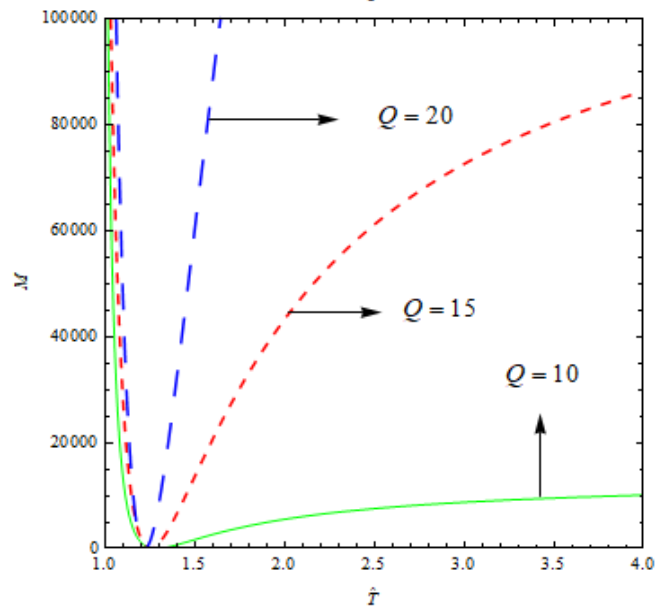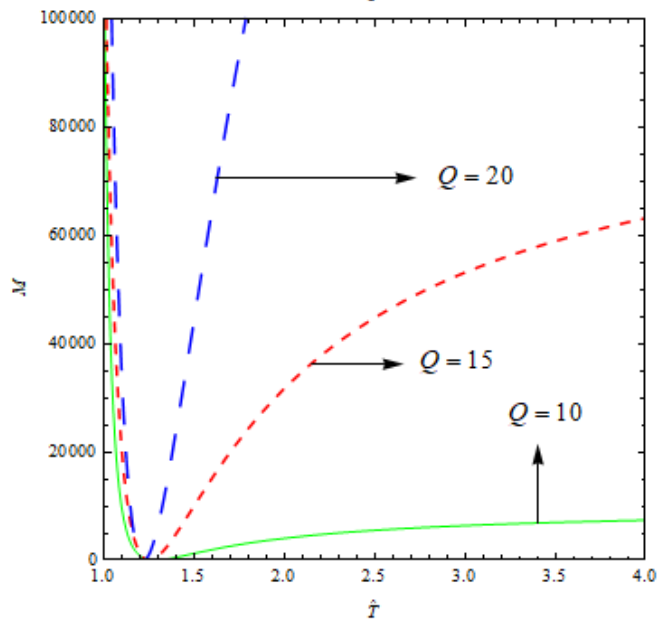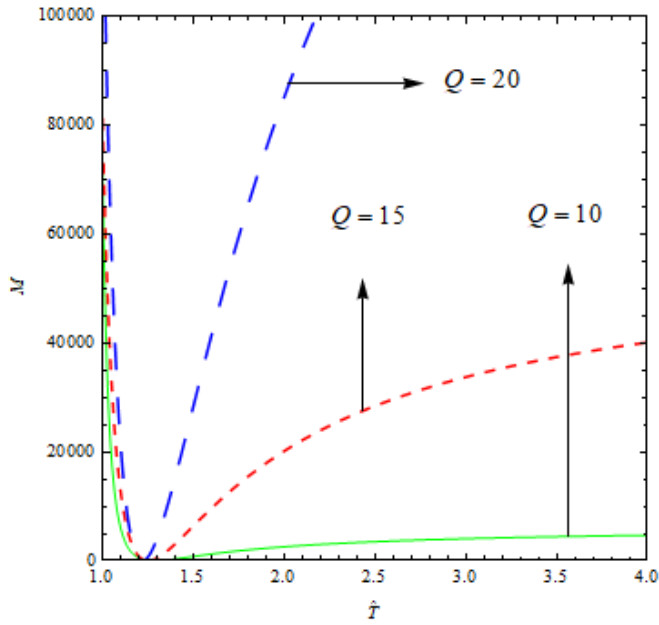
Fig. 4a-4c Thermal Marangoni number M versus thermal ratio $\hat{T}$ for different values of Chandrasekhar number Q

Fig. 5a-5c Thermal Marangoni number M versus thermal ratio $\hat{T}$ for different values of viscosity ratio $\hat{\mu}$
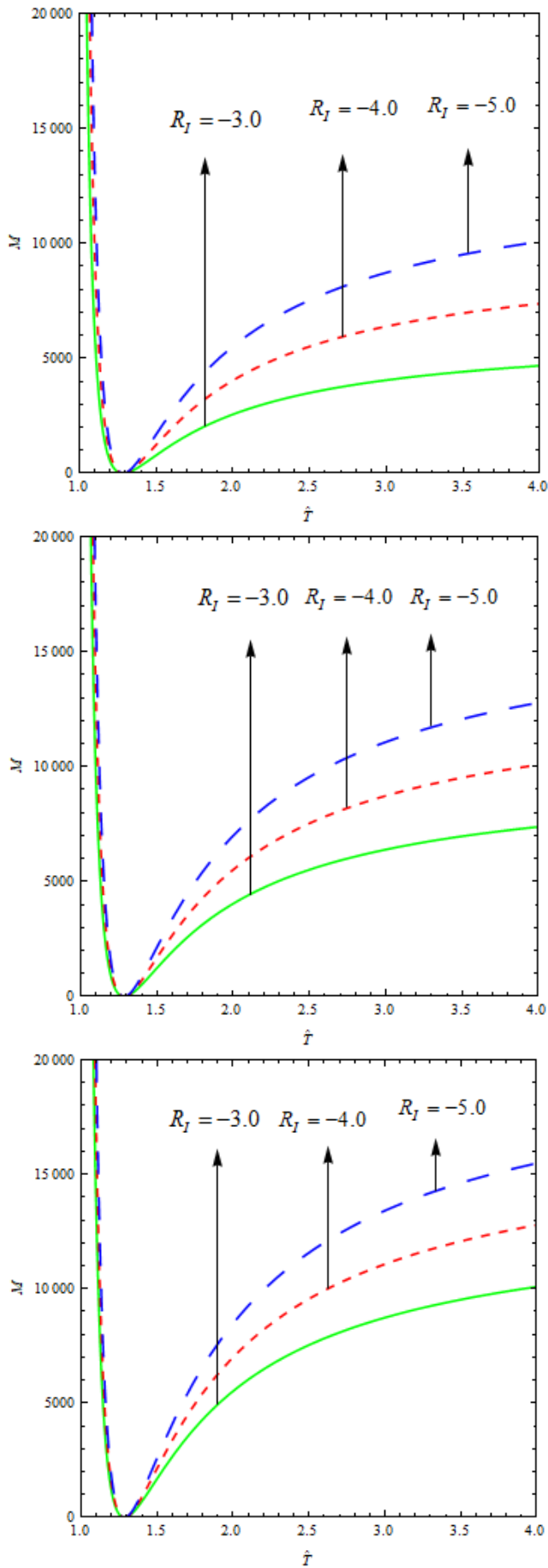
The effects of the viscosity ratio $\hat{\mu}$ on the thermal Marangoni number is shown in the Fig. 5a-5c, for all the three temperature profiles. The curves are diverging for larger values of thermal ratio, which indicates that the effect of $\hat{\mu}$ is effectual only for the higher values of thermal ratio and an enhance in the value of viscosity ratio $\hat{\mu}$, decreases the thermal Marangoni number M hence, the system can be stabilized by choosing smaller values of viscosity ratio $\hat{\mu}$.

The importance of internal Rayleigh number R_I on the Marangoni number is explained for all the three temperature profiles depicted the Fig. 6a-6c for R_I =-3, -4 and -5. Analogous effects are observed for the three profiles. The curves are slightly diverging indicating its prominence for composite layers with larger values of thermal ratio $\hat{T}$. Decreasing the values of R_I, the Marangoni number increases, hence the non-Darcy-Benard-magneto-surface tension driven convection can be delayed by decreasing the values of R_I. That is, heat absorption in the fluid layer favors stability of the system.

CONCLUSIONS

Following conclusions are drawn from this study:

i. The effects of the physical parameters considered in the study is similar to both uniform and non-uniform (parabolic and inverted parabolic) temperature gradients.

ii. The inverted parabolic temperature gradient is the exceedingly stable when compared to that of linear and parabolic temperature gradients.

iii. Non-Darcy-Benard-magneto-surface tension driven convection can be deferred by increasing the values of porous parameter and Chandrasekhar number.

iv. Non-Darcy-Benard-magneto-surface tension driven convection can be preponed by choosing larger values of the horizontal wavenumber a and viscosity ratio $\hat{\mu}$.

v. The presence of heat sink in the fluid layer postpones non-Darcy-Benard-magneto-surface tension driven convection whereas there is no effect of internal Rayleigh number R_{Im} on the same.

Fig. 6a-6c Thermal Marangoni number M versus thermal ratio $\hat{T}$ for different values of internal Rayleigh number R_I

REFERENCES

Ahmed Kadhim Hussein., M. A. Y. Bakier, Mohamed Bechir Ben Hamida, S. Sivasankaran., 2016. Magneto-hydrodynamic natural convection in an inclined T-shaped enclosure for different nanofluids and subjected to a uniform heat source, *Alexandria Engineering Journal*, 55(3), 2157-2169.

Bhadauria, B S., 2012. Double diffusive convection in a saturated anisotropic porous layer of micropolar fluid with heat source. *Transport in Porous Media*, 92, 299-320.

Chedsey, H. A., Hurle, D. T. J., 1966. Avoidance of growth-striae in semiconductor and metal crystals grown by zone melting techniques, *Nature*, 210 933-934.

Cookey, C., Omubo-Pepple, V. B., Obi, B. I., Eze, L C., 2010. Onset of thermal instability in a low Prandtl number fluid with internal heat source in a porous medium. *American Journal of Scientific and Industrial Research*, 1, 18-24.

Dileep Kumar, A.K. Singh, 2016. Effects of heat source/sink and induced magnetic field on natural convective flow in vertical concentric annuli, *Alexandria Engineering Journal*, 55, no.4, 3125-3133.

Fagbade, A. I., Falodun, B. O., Omowaye, A. J., 2018. MHD natural convection flow of viscoelastic fluid over an accelerating permeable surface with thermal radiation and heat source or sink: Spectral Homotopy Analysis Approach, *Ain Shams Engineering Journal*, 9(4), 1029-1041.

Girish, N., Sankar, M., Keerthi Reddy., 2019. Analysis of fully developed mixed convection in open-ended annuli with viscous dissipation *Journal of Thermal Analysis and Calorimetry*, https://doi.org/10.1007/s10973-019-09120-9.

Grosan, T., Revnic, C., Pop, I., Ingham, D. B., 2009. Magnetic field and internal heat generation effects on the free convection in a rectangular

cavity filled with a porous medium. *International Journal of Heat and Mass Transfer*, 52(5-6), 1525-1533.

Herron, I., 2001. Onset of convection in a porous medium with internal heat source and variable gravity. *Int. J. Eng. Sci.*, 39 (2), 201-208.

Jawdat, J. M., Hashim, I., 2010. Low Prandtl number chaotic convection in porous media with uniform internal heat generation, *International Communications in Heat and Mass Transfer*, 37(6), 629–636.

Joshi, M. V., Gaitonde, U. N., Mitra, S. K., 2006. Analytical study of natural convection in a cavity with volumetric heat generation, *ASME. J. Heat Transfer,* 128(2), 176-182.

Khalili, A., Shivakumara, I. S., 1998. Onset of convection in a porous layer with net through-flow and internal heat generation, *Physics of Fluids*, 10 (1), 315.

Khalili A., Shivakumara, I. S., Huettel, M., 2002. Effects of through-flow and internal heat generation on convective instabilities in an anisotropic porous layer, *Journal of Porous Media*, 5(3), 181-198.

Naveen Dwivedi., Ashok kumar Singh., 2020. Influence of Hall current on hydromagnetic natural convective flow between two vertical concentric cylinders in presence of heat source/sink, *Heat Transfer,* 49(3), 1402-1417.

Nouri-Borujerdi, A., Noghrehabadi, A. R., Rees, D.A.S., 2008. Influence of Darcy number on the onset of convection in porous layer with a uniform heat source, *International Journal of Thermal Sciences*, 47, 1020-1025.

Om Prakash Keshri., Anand Kumar., Vinod K.Gupta., 2019. Effect of internal heat source on magneto-stationary convection of couple stress fluid under magnetic field modulation, *Chinese Journal of Physics*, 57, 105-115.

Parthiban, C., Patil, P. R., 1997. Thermal instability in an anisotropic porous medium with internal heat source and inclined temperature gradient, *Int. Commun. Heat Mass Transfer*, 24(7), 1049-1058.

Ramesh, G. K., K. Ganesh Kumar., B. J. Gireesha., S. A. Shehzad., F. M. Abbasi., 2018. Magnetohydrodynamic nanoliquid due to unsteady contracting cylinder with uniform heat generation/absorption and convective condition, *Alexandria Engineering Journal*, 57 (4), 3333-3340.

Rao, Y.F., Wang, B. X. 1991. Natural convection in vertical porous enclosures with internal heat generation. *International Journal of Thermal Sciences*, 34, 247-252.

Rees, D A S., Pop, I., 1995. Free convection induced by a vertical wavy surface with uniform heat flux in a porous medium. *ASME Journal of Heat Transfer*, 117, 547-550.

Rionero, S., Straughan, B., 1990. Convection in a porous medium with internal heat source and variable gravity effects, *International Journal of Engineering Science*, 28(6), 497-503.

Sankar, M., Venkatachalappa, M., Shivakumara, I. S., 2006. Effect of magnetic field on natural convection in a vertical cylindrical annulus, *International Journal of Engineering science*, 44(20), 1556-1570.

Sankar, M., YoungyongPark, Lopez, J. M., YounghaeDo., 2011a. Numerical study of natural convection in a vertical porous annulus with discrete heating, *International Journal of Heat and Mass Transfer*, 54(7-8), 1493-1505.

Sankar, M., Venkatachalappa, M., YounghaeDo., 2011b. Effect of magnetic field on the buoyancy and thermocapillary driven convection of an electrically conducting fluid in an annular enclosure, *International Journal of Heat and Fluid flow*, 32(2), 402-412.

Sankar, M., Junpyo Park, Dongseok Kim., YounghaeDo., 2013. Numerical study of natural convection in a vertical porous annulus with an internal heat source: Effect of of discrete heating, *Numerical Heat Transfer, Part A: Applications*, 63(9), 687-712.

Sharma, P. R., Sharad Sinha., R. S. Yadav., Anatoly N. Filippov., 2018. MHD mixed convective stagnation point flow along a vertical stretching sheet with heat source/sink*, International Journal of Heat and Mass Transfer*, 117, 780-786.

Siddheshwar, P.G., Vanishree, R.K., 2018. Lorenz and Ginzburg Landau equations for thermal convection in a high porosity medium with heat source, *Ain Shams Engineering Journal*, 9, 1547-1555.

Sumithra, R., R.K. Vanishree., N. Manjunatha., 2020. Effect of constant heat source / sink on single component Marangoni convection in a composite layer bounded by adiabatic boundaries in presence of uniform \& non uniform temperature gradients, *Malaya Journal of Matematik*, 8(2), 306-313.

Sumithra, R., N. Manjunatha., 2020. Effects of Heat Source/ Sink and non uniform temperature gradients on Darcian-Benard-Magneto-Marangoni convection in composite layer horizontally enclosed by adiabatic boundaries, *Malaya Journal of Matematik*, 8 (2), 373-382.

Utech, H. P., Fleming, M. C., 1966. Elimination of solute banding in indium antimonide crystals by growth in a magnetic field, *Journal of Applied Physics*, 37, 2021.

Vadasz P., 2008. *Emerging topics in heat and mass transfer in porous media*, Springer, New York.